

Magnetic field tunable spectral response of kinetic inductance detectors

F. Levy-Bertrand,^{1,2,a)} M. Calvo,^{1,2} U. Chowdhury,^{1,2} A. Gomez,³ J. Goupy,⁴ and A. Monfardini^{1,2}

¹⁾Univ. Grenoble Alpes, CNRS, Grenoble INP, Institut Néel, 38000 Grenoble, France

²⁾Groupement d'Intérêt Scientifique KID, Grenoble and Saint Martin d'Hères, France

³⁾Centro de Astrobiología (CSIC-INTA), Ctra. Torrejón-Ajalvir km.4, 28850 Torrejón de Ardoz, Spain

⁴⁾CEA/DRF/IRIG – Grenoble - France

We tune the onset of optical response in aluminium kinetic inductance detectors from a natural cutoff frequency of 90 GHz to 60 GHz by applying an external magnetic field. The change in spectral response is due to the decrease of the superconducting gap, from 90 GHz at zero magnetic field to 60 GHz at a magnetic field of around 3 mT. We characterize the variation of the superconducting gap, the detector frequency shift and the internal quality factor as a function of the applied field. In principle, the magnetic field tunable response could be used to make spectroscopic measurements. In practice, the internal quality factor behaves hysteretically with the magnetic field due to the presence of vortices in the thin superconducting film. We conclude by discussing possible solutions to achieve spectroscopy measurements using kinetic inductance detectors and magnetic field.

Kinetic Inductance Detectors (KID), based on planar superconducting resonators¹, are popular detectors for astrophysical observations^{2,3} and interesting devices for physics studies⁴⁻⁹. One of the current challenges in millimetre astrophysics observations is to achieve a given degree of spectral resolution without sacrificing the large field-of-view of the current cameras. Here we explore a solution to achieve that goal by tuning the spectral response of KID with an external magnetic field. We present the first demonstration of the optical response of KID under a variable magnetic field. We also evaluate the effects of the applied magnetic field on the resonators quality factors and conclude by discussing future improvements of our initial KID design.

KID are a particular implementation of superconducting resonators. They are planar LC -resonant circuits made of superconductor thin films deposited on an insulating substrate, optimized for photon detection. The photon detection principle consists in monitoring the resonance frequency shift that is proportional to the incident power. Incident radiation breaks down Cooper pairs, generating quasi-particles and modifying the kinetic inductance resulting in an shift of the resonance frequency $f = 1/(2\pi\sqrt{LC})$ where C is the capacitance and $L = L_K + L_G$ is the total inductance, i.e. the sum of the kinetic and geometric inductances. The internal quality factor of the resonator decreases with the number of generated quasi-particles.

Figure 1 shows a schematic view of the experimental setup. The array of KID is made of a 200 nm aluminum film deposited on a high-resistivity silicon wafer. Four wire resistivity measurements performed on the same 200 nm aluminum film give a critical temperature $T_c \sim 1.2$ K and a perpendicular critical field $H_c \sim 4.5$ mT. Each KID is coupled via its inductor to the readout line. The inductor L is a Hilbert shape, sensitive to all in-plane polarization¹⁵. The lines are 4 μm wide. A magnetic field is applied perpendicular to the KID using a custom Helmholtz coil. The KID and the coil are cooled to approximately 100 mK in a dilution refrigerator with optical

access. Illumination is controlled by a Martin-Puplett spectrometer¹⁶ at room temperature and reaches the KID through a suitable series of optical filters and lenses¹⁷.

The bottom panel of figure 1 displays the measured spectral response of KID as a function of the incident optical frequency at different magnetic fields. The response extends from the 2Δ superconducting gap up to the low-pass filter frequency (180 GHz). At zero magnetic field the 2Δ superconducting gap equals 90 GHz, in agreement with the BCS-value $3.52k_B T_c/h \sim 88$ GHz. When increasing the magnetic field the 2Δ -gap decreases, increasing the band response from 90-180 GHz to 60-180 GHz at about 3 mT. The level of noise in the spectra, observable outside the response band, below 2Δ and above 180 GHz, increases with the magnetic field. Within the limits of noise and measurement accuracy, about ~ 1 GHz resolution for the optical frequency, the common-band response appears identical. So, in principle, by subtracting the response measured at 3 mT from that measured at zero magnetic field, we could obtain the response of the 60-90 GHz band. Extrapolating a little further, subtracting the responses measured at very close magnetic fields would give access to the response of a highly resolved spectral band: at 2 mT, a 0.001 mT step, would give a spectral resolution $R = \nu/\Delta\nu$ of about 8000 at 80 GHz (e.g. a spectral band of 0.01 GHz).

In practice, it is not so straightforward to access the spectroscopic signal. In a magnetic field, the frequency shift is due both to changes of the optical load, the signal of interest, and of the magnetic field. The latter are due to variations in the kinetic inductance L_k , resulting from the change of the 2Δ superconducting gap as $L_K = \hbar R_\square/(\pi\Delta)$ where R_\square is the sheet resistance in the normal state¹⁸.

Figure 2 illustrates the frequency variations due to both the magnetic field and the change in optical load. The figure shows Vector Network Analyser (VNA) response of a KID under two optical loads and two magnetic fields. The red and blue curves correspond, respectively, to measurements under a high or low optical load, with the 300 K window of the cryostat either closed by a dark plastic cap or closed by a mirror. The dark plastic cap acts as blackbody source at about 300 K ($T_{bb} \sim 300$ K). The mirror, which reflects the emission from the coldest stages of the cryostat, acts as a very cold black-

^{a)}Electronic mail: florence.levy-bertrand@neel.cnrs.fr

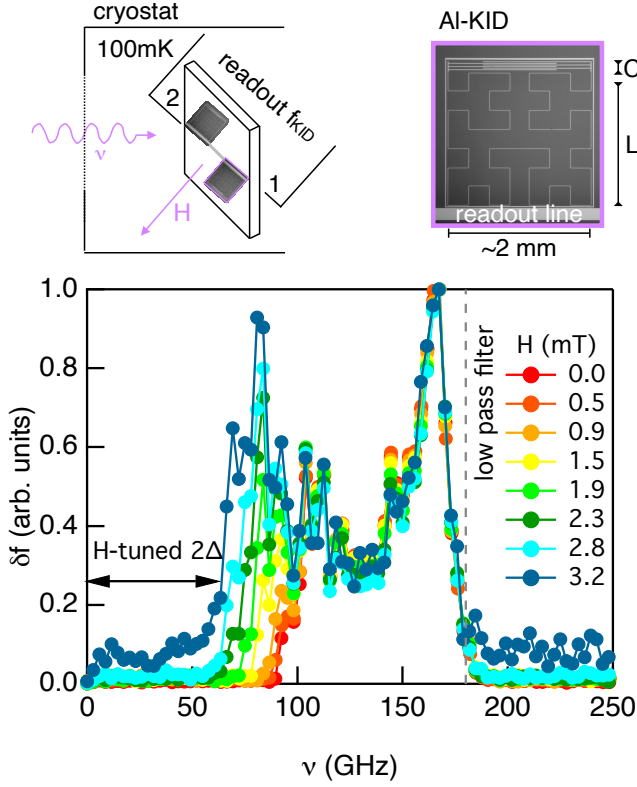


FIG. 1. **Magnetic field tunable spectral response of KID.** *Top* Experimental set-up and picture of a KID. The magnetic field is applied perpendicularly to the array. The illumination is controlled by a Martin-Puplett spectrometer at room temperature and reaches the array through a series of optical filters and lenses. *Bottom* Spectral response of KID to different magnetic fields: frequency shift of KID as a function the incident optical frequency. The low cut-off optical frequency corresponds to the 2Δ superconducting gap, which varies as a function of the magnetic field.

body source at about 0 K ($T_{bb} \sim 0$ K). Varying the magnetic field from 0 to 2.7 mT, the resonance frequency shifts by about 2 MHz (from left to right panel). Due to the optical signal, the resonance frequency shifts by 6 kHz at 0 mT and by 50 kHz at 2.7 mT.

To access the absolute spectroscopic signal preliminary calibrations in magnetic field are required. Figure 3 shows the variation of the superconducting gap, the frequency and the quality factor of KID with respect to the magnetic field. Within the errors bars both the 2Δ superconducting gap and the $\delta f/f$ relative frequency shift remain identical while ramping up and down the magnetic field. The magnetic field dependence of the superconducting gap follows the following formula valid for thin film¹⁹ (i.e. for $d/\lambda \ll 1$ where d is the thickness and λ is the magnetic penetration depth):

$$\Delta(H) = \Delta_0 \sqrt{1 - \left(\frac{H}{H_c}\right)^2} \quad (1)$$

where $\Delta_0 \sim 90$ GHz is the gap at zero magnetic field and

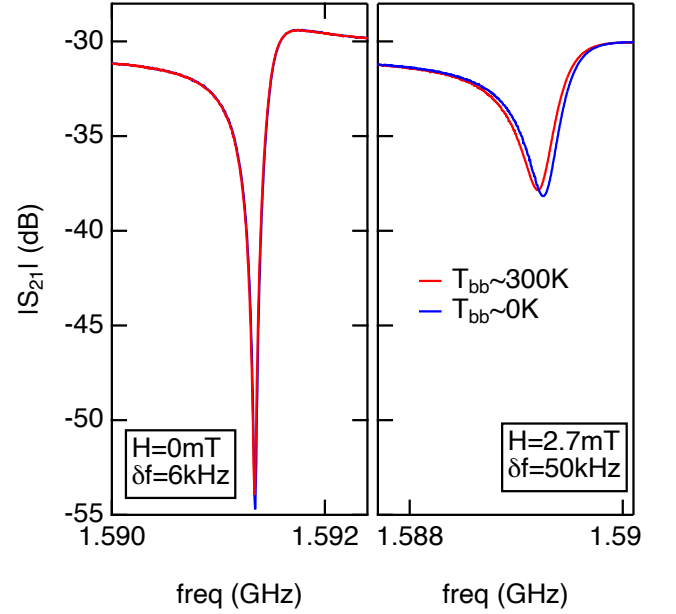


FIG. 2. **Magnetic field variation of the VNA response of a KID.** Measurements were done under two optical loads. Red curves for a large optical load: a black body source at about 300 K, $T_{bb} \sim 300$ K. Blue curves for a small optical load: a black body source at about 0 K, $T_{bb} \sim 0$ K. *Left* At zero magnetic field, the resonance is deep ($Q_i \sim 6e4$) and shifts by 6 kHz due to the variation in optical load. *Right* At almost 3 mT, the resonance is broad ($Q_i \sim 6e3$) and shifts by 50 kHz.

$H_c \sim 4.5$ mT is the critical field. The relative frequency shift under an almost constant small optical load is adjusted with the following formula valid for $\delta f \ll f$:

$$\frac{\delta f(H)}{f} = -\frac{\alpha_0}{2} \left[1 - \sqrt{1 - \left(\frac{H}{H_c}\right)^2} \right] \quad (2)$$

where $\alpha_0 = L_K^0 / (L_K^0 + L_G) \sim 1.4\%$ is the ratio of the kinetic inductance over the total inductance at zero magnetic field. The expression¹ is the usual, $\delta f/f = -\alpha/2 \times \delta L_k / L_k$, with the magnetic field dependence of L_K inserted. The value of α is in agreement with the ones estimated from the actual resonance frequency $f_{L_K+L_G}$, the resonance frequency simulated with the SONNET software^{10,11} without any kinetic inductance f_{L_G} and the following formula $\alpha = 1 - (f_{L_K+L_G}/f_{L_G})^2$, resulting in $\alpha \sim 1 - 4\%$. The value of α is low because the kinetic inductance of a 200 nm thick film of aluminum is small^{12,13}. The internal quality Q_i strongly varies with the magnetic field from about $10^6 - 10^5$ down to 10^3 and its value depends on the history of the magnetic field. This behavior is due to the presence of vortices in the resonator meander. The vortices are in the so-called plastic regime, in which they are alternatively pinned and mobile when sweeping the magnetic field^{20,21}. Vortices develop in aluminum thin films because they are type-II superconductors contrary to bulk aluminum^{13,14}.

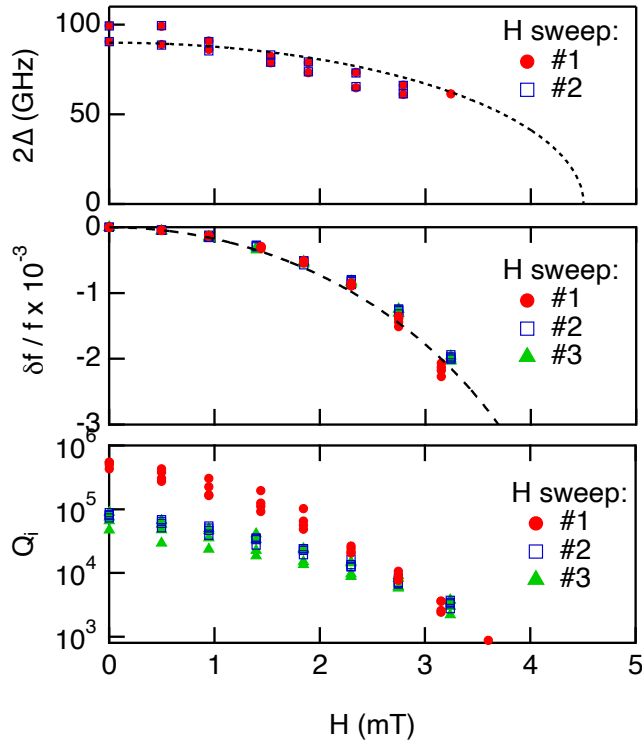


FIG. 3. **Magnetic field variation of the superconducting gap, the frequency and the quality factor of KID.** The different points for the same field and field sweep are the response of the different KID. The change of the 2Δ superconducting gap and of the $\delta f/f$ relative frequency shift with magnetic field are identical (within error bars) for the different magnetic sweeps. The dash lines are plots of equations (1) and (2). The Q_i internal quality factor depends on the history of the magnetic field.

To achieve spectroscopy using kinetic inductance detectors and magnetic field the first point to address is the vortex issue. The theory predicts that in thin superconducting films, vortices develop above a magnetic field perpendicular to the films $H_0 = \pi\Phi_0/(4w^2)$ where Φ_0 is the quantum of magnetic flux and w is the width of the superconducting line²². Experiments on 200 nm thick Nb superconducting lines validate the formula²³, and, show that the critical field for the vortex nucleation, H_0 drops drastically from about 200 mT in bulk Nb to below 1 mT for a 200 nm thick Nb film. For superconducting thin films, the width of the lines must be of the order of 500 nm to avoid the formation of vortices up to 5 mT. Thus, future developments of spectroscopy using kinetic inductance detectors and magnetic field requires a new KID design and e-beam lithography.

An other point to address is the magnetic field generation. The diameter of the magnetic coil must scale up with the diameter of the field of view which is proportional to the focal plane diameter. One solution is to implement a large standard coil at room temperature, around the cryostat. The magnetic field at the center of the coil is $H = \mu_0 IN/d$ where μ_0 is the

vacuum permittivity, I is the current, N is the number of turns and d is the diameter of the coil. For a diameter of 30 cm, a current of 1 A, and 3000 turns, the magnetic field equals 6 mT. This solution is the simplest from a cryogenic point of view, but the magnetic field on the KID may not be sufficiently homogeneous.

We tune the spectral response of kinetic inductance detectors with a magnetic field. The change in spectral response is due to the decrease of the superconducting gap when increasing the magnetic field. Our results suggest that it may be possible to achieve high-resolution spectroscopy over a wide field of view using KID and a magnetic field. The main pending limitation is the formation of vortices in the lines of the KID. This can be solved by reducing the lines width. The spectral resolution could reach several thousands depending also on the superconducting gap steepness. The spectral bands could be adjusted with the superconducting material and the magnetic field. Aluminum films with a critical temperature of $T_c \sim 1.2$ K and $H_c \sim 5$ mT give access to the relevant 50-100 GHz band. Tantalum with a critical temperature of $T_c \sim 4.5$ K and $H_c \sim 80$ mT could, in principle, give access to a 200-400 GHz band.

We acknowledge the contribution of G. Donnier-Valentin and of T. Gandit, respectively, for the design and for the realization of the Helmholtz superconducting coil. We acknowledge the contribution of O. Bourrion for the electronic acquisition. We thank B. Sacépé for excellent discussions. We acknowledge the overall support of the Cryogenics and Electronics groups at Institut Néel and LPSC. This work has been partially supported by the French National Research Agency through the LabEx FOCUS Grant No. ANR-11-LABX-0013 and the EU's Horizon 2020 research and innovation program under Grant Agreement No. 800923 (SUPERTED). A. G. acknowledges financial support from PID2022-137779OB-C41 funded by the Spanish MCIN/AEI/10.13039/501100011033.

The data that support the findings of this study are available from the corresponding author upon reasonable request.

REFERENCES

- ¹P. K. Day, H. G. LeDuc, B. A. Mazin, A. Vayonakis, and J. Zmuidzinas, *A Broadband Superconducting Detector Suitable for Use in Large Arrays*, *Nature* 425, 817 (2003).
- ²CONCERTO collaboration, *A wide field-of-view low-resolution spectrometer at APEX: Instrument design and scientific forecast*, *Astronomy & Astrophysics* 642, A60 (2021).
- ³NIKA2 collaboration, *Calibration and performance of the NIKA2 camera at the IRAM 30-m Telescope*, *Astronomy & Astrophysics* 637, A71 (2020).
- ⁴B. Aja et al., *The Canfranc Axion Detection Experiment (CADEX): Search for Axions at 90 GHz with Kinetic Inductance Detectors*, *J. Cosmol. Astropart. Phys.* 2022, 044 (2022).
- ⁵A. Cruciani et al., *BULLKID: Monolithic Array of Particle Absorbers Sensed by Kinetic Inductance Detectors*, *Applied Physics Letters* 121, 213504 (2022).
- ⁶F. Levy-Bertrand et al., *Electrodynamics of Granular Aluminum from Superconductor to Insulator: Observation of Collective Superconducting Modes*, *Phys. Rev. B* 99, 094506 (2019).
- ⁷P. J. de Visser, S. J. C. Yates, T. Guruswamy, D. J. Goldie, S. Withington, A. Neto, N. Llombart, A. M. Baryshev, T. M. Klapwijk, and J. J. A. Baselmans,

- The Non-Equilibrium Response of a Superconductor to Pair-Breaking Radiation Measured over a Broad Frequency Band*, Applied Physics Letters 106, 252602 (2015).
- ⁸E. F. C. Driessen, P. C. J. J. Coumou, R. R. Tromp, P. J. de Visser, and T. M. Klapwijk, *Strongly Disordered TiN and NbTiN S-Wave Superconductors Probed by Microwave Electrodynamics*, Phys. Rev. Lett. 109, 107003 (2012).
- ⁹L. Grünhaupt, N. Maleeva, S. T. Skacel, M. Calvo, F. Levy-Bertrand, A. V. Ustinov, H. Rotzinger, A. Monfardini, G. Catelani, and I. M. Pop, *Loss Mechanisms and Quasiparticle Dynamics in Superconducting Microwave Resonators Made of Thin-Film Granular Aluminum*, Phys. Rev. Lett. 121, 117001 (2018).
- ¹⁰J. C. Rautio and R. F. Harrington, *An Electromagnetic Time-Harmonic Analysis of Shielded Microstrip Circuits*, IEEE Trans. Microwave Theory Techn. 35, 726 (1987).
- ¹¹SONNET, Sonnet Software, Liverpool, NY, 2005.
- ¹²A. Adane, C. Boucher, G. Coiffard, S. Leclercq, K. F. Schuster, J. Goupy, M. Calvo, C. Hoarau, and A. Monfardini, *Crosstalk in a KID Array Caused by the Thickness Variation of Superconducting Metal*, J Low Temp Phys 184, 137 (2016).
- ¹³D. López-Núñez, Q. P. Montserrat, G. Rius, E. Bertoldo, A. Torras-Coloma, M. Martínez, and P. Forn-Díaz, *Magnetic Penetration Depth of Aluminum Thin Films*, arXiv:2311.14119.
- ¹⁴M. Tinkham, *Introduction to Superconductivity*.
- ¹⁵A. Monfardini et al., *Latest NIKA Results and the NIKA-2 Project*, J Low Temp Phys 176, 787 (2014).
- ¹⁶Details on the Martin-Puplett spectrometer are in the Supplementary information of N. Maleeva et al., *Circuit Quantum Electrodynamics of Granular Aluminum Resonators*, Nat Commun 9, 3889 (2018).
- ¹⁷A. Monfardini et al., *A Dual-band Millimeter-wave Kinetic Inductance Camera for the IRAM 30 m Telescope*, The Astrophysical Journal Supplement Series 194, Number 2, 24 (2011).
- ¹⁸A. J. Annunziata, D. F. Santavicca, L. Frunzio, G. Catelani, M. J. Rooks, A. Frydman, and D. E. Prober, *Tunable Superconducting Nanoinductors*, Nanotechnology 21, 445202 (2010).
- ¹⁹D. H. Douglass, *Magnetic Field Dependence of the Superconducting Energy Gap*, Phys. Rev. Lett. 6, 346 (1961).
- ²⁰K. Borisov et al., *Superconducting Granular Aluminum Resonators Resilient to Magnetic Fields up to 1 Tesla*, Applied Physics Letters 117, 120502 (2020).
- ²¹C. Song, T. W. Heitmann, M. P. DeFeo, K. Yu, R. McDermott, M. Neeley, J. M. Martinis, and B. L. T. Plourde, *Microwave Response of Vortices in Superconducting Thin Films of Re and Al*, Phys. Rev. B 79, 174512 (2009).
- ²²G. M. Maksimova, *Mixed State and Critical Current in Narrow Semiconducting Films*, Phys. Solid State 40, 1607 (1998).
- ²³G. Stan, S. B. Field, and J. M. Martinis, *Critical Field for Complete Vortex Expulsion from Narrow Superconducting Strips*, Phys. Rev. Lett. 92, 097003 (2004).